Jour. Petrol. Soc. Korea
Vol. 5, No. 1, p. 35~51, 1996

Geochemistry and Petrogenesis of the Granitic Rocks in the Vicinity of the Mt. Sorak

Kyoung-Won Min[1] and Sung-Bum Kim[2]

[1]Department of Resources Engineering, Kangwon National University, Chuncheon 200-701
[2]Ssangyong Resources Development Co. Ltd., Donghae 240-350(deceased on Feb. 10, 1996)

ABSTRACT : The granitic rocks in the vicinity of the Mt. Sorak, the northeastern part of the NE-SW elongated Mesozoic granitic batholith in the Kyeonggi massif, consist of granodiorite, biotite granite, two-mica granite and alkali feldspar granite. Variations in major and most trace elemental abundances show a typical differentiation trend in a granitic magma. Granitic rocks all display a calc-alkaline trend in the AFM diagram. Also, in the ACF diagram discriminating between I- and S-type granitic rocks, granodiorite and most biotite granite in the southeastern area represent I-type and magnetite-series characteristics, while most biotite granite and two-mica granite in the northwestern area exhibit S-type and ilmenite-series ones. According to recent studies of the granitic rocks in the Inje-Hongcheon district, all the granitic rocks distributed in the northeastern part of the Kyeonggi massif have been classified as late Triassic to early Jurassic Daebo granite. With reference of the formerly published ages, an age of 125.6±4.4 Ma calculated by the slope in the plot of $^{87}Rb/^{86}Sr$-$^{87}Sr/^{86}Sr$ for the biotite granite samples from the southeastern area is inferred as an emplacement age for the granitic rocks in the vicinity of the Mt. Sorak. On the basis of elemental variations and Sr isotope compositions, an possible evolutional process for the granitic magmas in this area is suggested. The primary magma of I-type and magnetite-series generated about 125 Ma by partial melting of igneous originated crustal materials, might be emplaced and evolved through fractional crystallization, convection and assimilation of the surrounding Precambrian metasediments to become S-type and ilmenite-series in the outer area, and then solidified to granodiorite, biotite granite and two-mica granite. At the latest stage, the evolved hydrothermal solution altered the formerly solidified biotite granite to alkali feldspar granite and probably later local igneous activities affected the alkali feldspar granite again.

Key words : Mt. Sorak, granitic rocks, geochemistry, petrogenesis, fractional crystallization, assimilation

INTRODUCTION

The granitic rocks in the vicinity of the Mt. Sorak, the northeastern part of the Kyeonggi massif, were formerly grouped into the Cretaceous Bulgugsa granite (KIER, 1983). However, recent geochronological studies suggested that all the granitic rocks from the Inje-Hongcheon district have been formed during late Triassic to early Jurassic period on the basis of the Rb-Sr whole rock isochron of 212± 26.6 Ma for hornblende-biotite granodiorite (Jwa *et al.*, 1990). So, nowadays, all the granitic rocks distributed in the northeastern part of the Kyeonggi massif are classified as the Daebo granite. In this article, the age of the granitic rocks in the vicinity of the Mt. Sorak is reviewed with newly measured Rb-Sr isotope age and the formerly published radiometric ages, fission track ages for apatites, K-Ar ages for biotites and Rb-Sr ages for two points of biotite and whole rock (Choo *et al.*, 1982; Jin *et al.*, 1984). The granitic rocks in the study area is described in terms of petrog-

raphy and geochemistry in major and trace elements and Sr isotope. The evolutional process of the granitic rocks is also thoroughly discussed mainly in a viewpoint of elemental and Sr isotopic variations.

GEOLOGICAL SETTINGS

The study area is located the northeastern part of the NE-SW elongated Mesozoic batholith of granitic rocks distributed in the Kyeonggi massif. The area is mainly composed of Precambrian metasedimentary basement and Mesozoic granitic rocks (Fig. 1). The Precambrian basement, a part of the Kyeonggi metamorphic complex, is composed of banded gneiss, biotite gneiss, quartz-feldspathic gneiss and biotite schist. The granitic rocks consist of granodiorite, biotite granite, two-mica granite, alkali feldspar granite, leucocratic porphyritic granite and granitic porphyry. Because of their younger emplacement age and geochemical characteristics distinct from those of the other granites, leucocratic porphyritic granite and granitic porphyry are excluded in this article and will be separately dealt in a preparing paper. Granodiorite is distributed in the central part of the study area and near the Baekdamsa, and is coarse grained with porphyritic textures in some localities. Granodiorite contains characteristically biotite and hornblende in most rock samples. Biotite granite is a medium to coarse grained equigranular rock and shows gradual contact relations with two-mica granite and metamorphic country rocks. Migmatitic rocks are often observed along the boundary between biotite granite and country rocks. Fine to medium grained two-mica granite is distributed in the northwestern boundaries contacted with Precambrian basement. Alkali feldspar granite, which is mainly exposed along the road passing the Hangyeryeong, contains pinkish alkali feldspar. Recently all the granitic rocks in the Inje-Hongcheon district, southwestern extension of the study area, were interpreted to be emplaced during late Triassic to early Jurassic period (about 212Ma) (Jwa *et al.*, 1990).

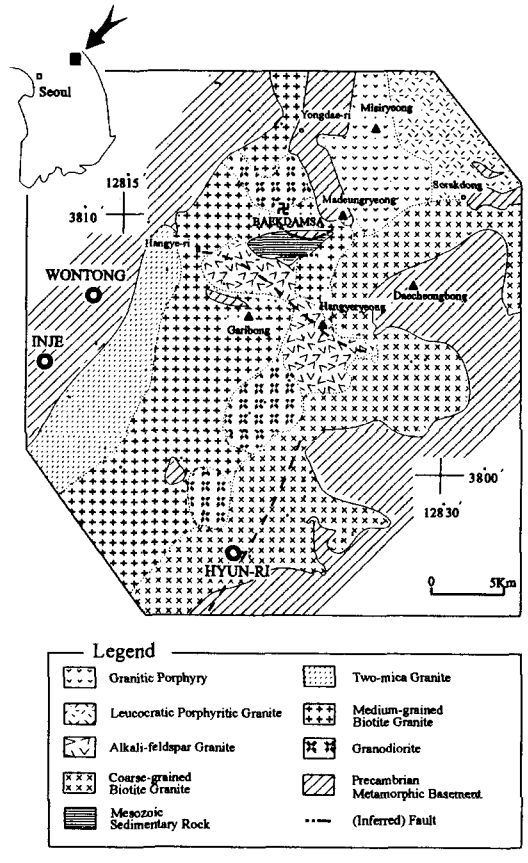

Fig. 1. Geologic map around the Mt. Sorak area.

PETROGRAPHIC DESCRIPTION OF THE GRANITIC ROCKS

The granitic rocks in the study area can be classified into granodiorite, biotite granite, two-mica granite, alkali feldspar granite, and additionally leucocratic porphyritic granite and granitic porphyry non-described in this paper. Granodiorite is generally coarse grained rock with some porphyritic feature of pale pinkish alkali feldspar phenocrysts and consists mainly of quartz, plagioclase, alkali feldspar, biotite, hornblende and minor minerals such as zircon, sphene, apatite and magnetite. Secondary minerals are sericite, chlorite, epidote, cal-

cite and pyrite. Plagioclase generally shows albite twin and is occasionally altered to sericite. Alkali feldspar is microperthite or microcline. Green hornblende occurs as prismatic or rhombic forms occasionally with lamella twinning. Greenish chlorite and some epidote are developed along the rim of hornblende. Biotite shows a strong pleochroism of greenish or brown to dark brown color under the microscope and is altered to chlorite along cleavage planes. Apatite, sphene and zircon occur generally in association with biotite.

Biotite granite is medium grained in the northwestern area and coarse grained in the southeastern area. The rock is composed mainly of quartz, plagioclase, alkali feldspar, biotite with minor muscovite, zircon, apatite and magnetite. Secondary products are sericite, chlorite, epidote, calcite and pyrite. Plagioclase exhibits Carlsbad-albite twinning and zonal features in some sections. Alkali feldspar is microperthite, microcline and orthoclase. Biotite shows a brown to dark brown pleochroism under the microscope. Poorly cleavaged muscovite is often found as a minor mineral.

Two-mica granite is fine to medium grained and equigranular, and consists of quartz, plagioclase, alkali feldspar, biotite, muscovite, zircon, apatite and secondary minerals such as sericite, chlorite, epidote, calcite and opaque minerals. Plagioclase has Carlsbad-albite or albite twin and often shows myrmekitic intergrowth texture. Alkali feldspar is mainly microperthite and microcline. Biotite showing brown to dark brown pleochroism has usually good cleavage with some bended crystals. Muscovite occurs as tabular forms and is closely associated with biotite. Zircon, apatite and opaques occur as minor minerals.

Alkali feldspar granite is wholly pinkish due to pinkish to reddish alkali feldspars and consists of microcline, quartz, plagioclase, biotite, chlorite, zircon, muscovite, magnetite. Alkali feldspar exhibits unclear looking probably due to numerous tiny inclusions and occurs as microperthite.

WHOLE ROCK GEOCHEMISTRY

Granitic rock specimens (Fig. 2) were analyzed for major and trace elements including rare earth elements (REE). Major element data were obtained by a combination of X-ray Fluorescence (XRF) method and gravimetric techniques at the Ssangyong Research Center (Table 1). Trace elements were determined by inductively coupled plasma - atomic emission spectrometry (ICP-AES), instrumental neutron activation analysis (INAA) and XRF at the Activation Laboratory Ltd., Canada (Table 1).

The Harker's diagrams of major oxide abundances versus SiO_2 contents reveal generally regular variation trends with somewhat scattered variations in FeO, Fe_2O_3 and MnO for all granitic rocks in this area (Fig. 3). With the increase of SiO_2 contents the contents of Al_2O_3, CaO, MgO, FeO, Fe_2O_3, TiO_2 and P_2O_5 decrease systematically, while K_2O content increases regularly and Na_2O content does not vary, which is a typical differentiation trend in a granitic

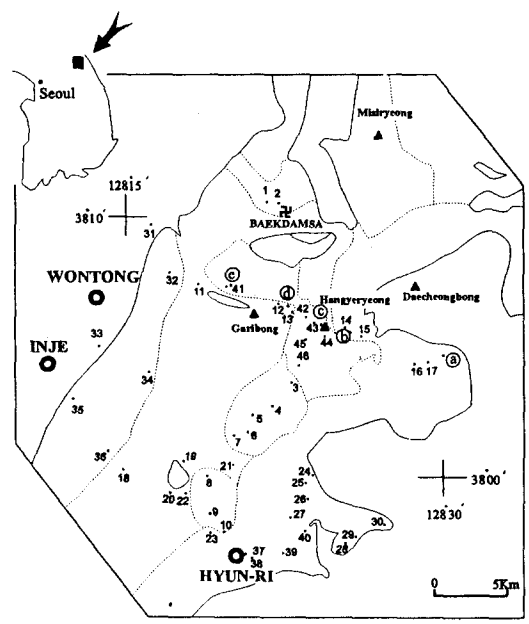

Fig. 2. Sample locations of the granitic rocks in the study area.

Table 1. Major element abundances(wt.%), trace element abundances(ppm) and CIPW norms.

Map No.	1	2	3	4	5	6	7	8	9	10	11
Field No.	SR-01-5	SR-01-3	SR-23	SR-24	SR-25	SR-35	SR-35-3	SR-37	SR-32	SR-30	SR-17
Rock type	GD	GD	GD	GD	GD	GD	GD	GD	GD	GD	MBG
SiO_2	63.53	65.87	60.10	68.24	68.76	64.54	62.78	67.41	59.49	62.08	72.58
TiO_2	0.67	0.59	0.58	0.34	0.40	0.56	0.59	0.47	0.83	0.53	0.28
Al_2O_3	15.55	15.72	17.52	15.64	16.14	15.82	16.01	15.89	17.58	17.53	13.74
Fe_2O	1.87	1.81	3.22	1.04	1.02	1.97	2.08	1.24	3.21	2.61	0.36
FeO	2.62	2.31	2.19	1.60	1.89	2.49	2.24	2.80	3.35	2.48	2.55
MnO	0.07	0.06	0.10	0.04	0.06	0.08	0.08	0.06	0.10	0.09	0.04
MgO	1.67	1.45	3.08	1.36	1.28	2.12	2.03	1.32	2.96	2.81	1.00
CaO	4.43	4.13	5.32	3.18	3.46	4.42	4.88	3.44	5.64	5.10	1.38
Na_2O	3.17	3.22	3.61	3.40	3.60	3.10	3.30	3.44	3.11	3.32	2.84
K_2O	2.98	3.55	1.68	3.08	2.64	2.52	2.50	3.12	2.02	2.08	4.04
P_2O_5	0.15	0.13	0.20	0.12	0.16	0.20	0.17	0.14	0.24	0.22	0.08
LOI	1.04	0.83	1.40	0.84	1.22	0.98	1.35	0.88	1.94	1.46	0.72
Total	97.75	99.67	99.00	98.88	100.63	98.80	98.01	100.21	10.47	100.31	99.61
Ba	849.0	961.0	866.0	818.0	730.0	718.0	780.0	820.0	918.0	900.0	658.0
Rb	103.0	123.0	62.0	90.0	92.0	81.0	80.0	125.0	85.0	69.0	184.0
Sr	425.0	400.0	600.0	444.0	466.0	472.0	533.0	410.0	515.0	544.0	168.0
Cr	107.0	120.0	150.0	95.0	110.0	110.0	128.0	100.0	110.0	150.0	130.0
Ga	26.0	28.0	17.0	19.0	19.0	20.0	24.0	20.0	17.0	21.0	16.0
Nb	13.0	12.0	9.0	6.0	7.0	10.0	10.0	10.0	6.0	7.0	19.0
Ni	41.0	45.0	59.0	33.0	48.0	41.0	47.0	52.0	57.0	54.0	49.0
Pb	7.0	9.0	11.0	15.0	13.0	11.0	5.0	16.0	9.0	8.0	32.0
Th	13.2	13.6	11.0	8.0	1.2	11.0	7.2	16.0	10.0	5.0	20.0
V	39.0	34.0	136.0	45.0	56.0	90.0	56.0	53.0	108.0	109.0	39.0
Y	22.0	21.0	16.0	8.0	12.0	16.0	20.0	4.0	20.0	20.0	20.0
Zn	66.0	58.0	89.0	62.0	5.0	80.0	57.0	78.0	88.0	70.0	59.0
Zr	196.0	164.0	144.0	110.0	336.0	172.0	135.0	157.0	181.0	151.0	136.0
Be	2.0	2.0	2.0	3.0	3.0	2.0	2.0	4.0	2.0	2.0	3.0
Co	9.1	8.2	18.0	6.6	7.4	11.0	9.6	8.6	14.0	15.0	9.7
Cs	1.4	1.7	5.1	1.2	2.4	2.0	1.1	3.7	2.7	1.5	4.3
Cu	5.0	4.0	11.0	2.0	2.0	6.0	7.0	11.0	8.0	4.0	19.0
Hf	4.2	4.2	5.5	4.5	5.1	5.3	3.6	4.9	5.4	4.7	6.3
Mo	7.0	5.0	2.0	2.0	4.0	6.0	6.0	5.0	4.0	3.0	9.0
Sc	8.4	7.2	17.0	4.3	5.0	9.4	8.7	8.3	13.0	13.0	6.6
Ta	0.8	0.8	0.3	0.9	1.3	1.1	0.6	0.9	0.3	0.9	2.0
U	1.1	2.0	0.6	1.6	1.9	1.1	1.3	3.2	1.3	0.9	6.1
CIPW NORMS											
qz	21.43	22.41	16.80	27.48	27.90	23.81	20.64	24.94	16.79	19.60	34.55
c	-	-	0.52	1.22	1.45	0.44	-	0.93	0.60	1.09	2.38
or	17.61	20.98	9.93	18.20	15.60	14.89	14.77	18.44	11.94	12.29	23.88
ab	26.82	27.25	30.80	28.77	30.46	26.23	27.92	29.11	26.32	28.01	24.03
an	19.40	17.96	25.09	14.99	16.12	20.62	21.49	16.15	26.41	23.87	6.32
wo	-	-	-	-	-	-	-	-	-	-	-
di-di	0.88	0.96	-	-	-	-	1.01	-	-	-	-
di-he	0.42	0.43	-	-	-	-	0.27	-	-	-	-
hy-en	3.75	3.18	7.67	3.39	3.19	5.28	4.59	3.29	7.37	7.00	2.49
hy-fo	2.07	1.66	0.59	1.59	2.08	2.17	1.42	3.45	2.31	1.69	4.00
mt	2.71	2.62	4.67	1.51	1.48	2.68	3.02	1.80	4.65	3.78	0.52
il	1.27	1.12	1.10	0.65	0.76	1.06	1.12	0.89	1.58	1.01	0.53
he	-	-	-	-	-	-	-	-	-	-	-
ap	0.36	0.03	0.47	0.28	0.38	0.47	0.40	0.33	0.57	0.52	0.19

GD:Granodiorite, MBG:Medium-grained Biotite Granite, TMG:Two-mica Granite,
CBG:Coarse-grained Biotite Granite, AFG:Alkali Feldspar Granite

Table 1. Continued.

Map No.	12	13	18	19	20	21	22	31	32	33	34
Field No.	SR-9	SR-19-2	SR-39	SR-38-1	SR-38	SR-36	SR-34	SR-01	SR-17-2	SR-27	SR-26
Rock type	MBG	MBG	MBG	MBG	MBG	MBG	MBG	TMG	TMG	TMG	TMG
SiO_2	73.90	68.56	69.32	72.20	69.98	73.30	72.97	72.85	70.36	70.14	72.16
TiO_2	0.22	0.41	0.34	0.29	0.18	0.16	0.10	0.19	0.34	0.24	0.24
Al_2O_3	14.36	15.30	16.13	13.21	14.98	13.92	15.03	14.13	13.55	14.02	14.92
Fe_2O	0.71	1.41	0.51	0.41	0.20	0.29	0.14	0.36	0.53	0.57	0.42
FeO	0.90	1.39	2.91	2.01	1.59	1.27	0.92	1.36	2.76	1.93	1.42
MnO	0.01	0.05	0.05	0.04	0.04	0.02	0.02	0.04	0.05	0.04	0.04
MgO	0.32	1.10	1.45	0.72	0.54	0.32	0.29	0.46	1.09	0.94	0.40
CaO	0.70	3.04	1.38	1.47	1.42	1.24	1.52	1.48	1.47	1.38	1.40
Na_2O	3.06	3.74	2.61	3.00	3.12	2.98	3.15	2.88	2.97	3.08	3.30
K_2O	5.50	3.37	4.16	4.37	4.64	5.00	5.64	5.80	3.85	4.00	4.88
P_2O_5	0.08	0.13	0.08	0.07	0.08	0.08	0.10	0.14	0.08	0.12	0.12
LOI	0.56	0.95	1.15	0.74	0.74	0.52	0.41	0.97	1.05	1.26	0.62
Total	100.32	99.45	100.09	98.53	97.51	99.10	100.29	100.66	98.10	97.72	99.92
Ba	1291.0	1177.0	783.0	603.0	682.0	710.0	1314.0	894.0	746.0	598.0	1004.0
Rb	165.0	95.0	192.0	213.0	208.0	207.0	136.0	209.0	189.0	175.0	175.0
Sr	268.0	545.0	190.0	209.0	210.0	196.0	283.0	251.0	200.0	144.0	270.0
Cr	120.0	130.0	120.0	119.0	86.0	88.0	74.0	160.0	142.0	120.0	55.0
Ga	15.0	27.0	18.0	27.0	17.0	35.0	14.0	19.0	28.0	20.0	17.0
Nb	8.0	8.0	10.0	19.0	12.0	14.0	4.0	11.0	19.0	18.0	10.0
Ni	52.0	42.0	51.0	52.0	42.0	37.0	27.0	37.0	60.0	50.0	24.0
Pb	25.0	11.0	29.0	26.0	36.0	31.0	41.0	33.0	21.0	26.0	29.0
Th	27.0	7.6	32.0	21.9	27.0	24.0	15.0	35.0	22.0	27.0	24.0
V	8.0	28.0	42.0	19.0	17.0	9.0	6.0	7.0	25.0	30.0	18.0
Y	14.0	19.0	50.0	28.0	28.0	8.0	22.0	6.0	38.0	4.0	12.0
Zn	37.0	45.0	74.0	46.0	59.0	46.0	15.0	32.0	43.0	56.0	48.0
Zr	165.0	167.0	157.0	159.0	86.0	106.0	48.0	121.0	289.0	110.0	184.0
Be	2.0	2.0	2.0	2.0	5.0	2.0	3.0	2.0	2.0	4.0	3.0
Co	3.2	5.3	13.0	4.4	5.9	2.8	2.2	4.1	8.3	8.0	3.7
Cs	2.0	2.1	7.1	3.8	4.8	3.7	2.9	2.2	3.6	6.2	3.0
Cu	6.0	7.0	9.0	5.0	2.0	1.0	1.0	6.0	13.0	10.0	1.0
Hf	6.4	3.3	5.3	3.4	4.3	5.0	2.4	5.6	5.5	4.8	6.3
Mo	7.0	6.0	5.0	9.0	2.0	5.0	4.0	6.0	7.0	2.0	3.0
Sc	3.8	4.4	9.4	4.3	3.9	2.8	1.9	2.6	6.5	5.6	3.9
Ta	0.3	0.5	1.1	1.1	1.7	1.3	1.0	1.2	1.0	1.7	1.1
U	1.6	1.2	8.2	8.6	11.0	6.3	3.8	3.6	5.7	5.9	4.8
CIPW NORMS											
qz	32.97	25.75	31.29	32.66	29.30	33.07	28.99	29.54	31.90	31.64	30.14
c	2.29	0.28	5.02	1.04	2.43	1.54	1.22	0.76	2.02	2.40	1.95
or	32.50	19.92	14.58	25.83	27.42	29.55	33.33	32.48	22.75	23.64	28.84
ab	25.89	31.65	22.09	25.39	26.40	25.22	26.66	24.37	25.13	26.06	27.92
an	2.95	14.23	6.32	6.84	6.52	5.63	6.89	6.43	6.77	6.06	6.16
wo	-	-	-	-	-	-	-	-	-	-	-
di-di	-	-	-	-	-	-	-	-	-	-	-
di-he	-	-	-	-	-	-	-	-	-	-	-
hy-en	0.80	2.74	3.61	1.79	1.35	0.80	0.72	1.15	2.72	2.34	1.00
hy-fo	0.72	0.80	4.45	2.94	2.53	1.87	1.45	1.96	4.16	2.75	1.94
mt	1.03	2.04	0.74	0.61	0.29	0.42	0.20	0.52	0.77	0.83	0.61
il	0.42	0.78	0.65	0.55	0.34	0.30	0.19	0.36	0.65	0.46	0.46
he	-	-	-	-	-	-	-	-	-	-	-
ap	0.19	0.31	0.19	0.17	0.19	0.19	0.24	0.33	0.19	0.28	0.28

Table 1. Continued.

Map No.	35	36	14	15	16	17	23	24	25	26	27	28
Field No.	SR-41	SR-40	SR-16-3	SR-16	SR-15	SR-14	SR-31	J-11	J-10	J-09	J-06	SR-28-3
Rock type	TMG	TMG	CBG	CBG	CBG	CBG	CBG	CBG	CBG	CBG	CBG	CBG
SiO_2	73.16	73.80	74.55	74.28	71.02	72.62	72.26	72.40	73.78	72.85	71.68	68.32
TiO_2	0.22	0.08	0.17	0.12	0.18	0.16	0.08	0.19	0.18	0.15	0.18	0.34
Al_2O_3	13.60	14.16	13.01	13.48	14.94	13.88	14.08	13.69	13.54	13.70	13.62	14.61
Fe_2O	0.29	0.07	1.13	0.42	0.87	0.90	0.17	1.21	1.23	1.14	1.23	1.21
FeO	2.20	0.87	0.45	1.33	0.93	0.90	0.26	0.77	0.60	0.45	0.50	1.75
MnO	0.04	0.02	0.11	0.12	0.08	0.10	0.02	0.06	0.06	0.05	0.05	0.06
MgO	0.88	0.28	0.19	0.18	0.42	0.38	0.22	0.38	0.35	0.26	0.38	1.30
CaO	1.16	1.32	1.00	0.94	1.86	1.50	1.04	1.56	0.32	1.35	1.05	3.23
Na_2O	2.52	3.24	3.75	3.68	3.94	3.78	3.42	3.61	3.57	3.75	3.53	2.94
K_2O	3.80	4.64	4.58	4.68	3.92	4.20	5.12	4.35	4.41	4.42	4.59	4.25
P_2O_5	0.12	0.08	0.05	0.08	0.08	0.08	0.04	0.12	0.07	0.06	0.07	0.09
LOI	0.84	0.50	0.49	0.54	0.68	2.20	0.78	0.69	0.54	0.59	1.34	1.24
Total	98.83	99.06	99.48	99.85	98.92	100.70	97.49	99.03	99.65	98.77	98.22	99.34
Ba	518.0	572.0	358.0	474.0	1134.0	674.0	428.0	676.0	491.0	577.0	717.0	785.0
Rb	170.0	156.0	158.0	174.0	147.0	183.0	220.0	199.0	173.0	198.0	171.0	137.0
Sr	130.0	148.0	122.0	130.0	402.0	292.0	132.0	223.0	199.0	152.0	243.0	310.0
Cr	110.0	72.0	101.0	110.0	77.0	110.0	75.0	89.1	85.0	89.3	111.0	155.0
Ga	16.0	13.0	20.0	16.0	15.0	14.0	18.0	23.0	22.0	23.0	20.0	21.0
Nb	14.0	6.0	21.0	22.0	14.0	19.0	8.0	16.0	14.0	14.0	13.0	12.0
Ni	44.0	38.0	37.0	42.0	41.0	53.0	41.0	37.0	32.0	30.0	42.0	59.0
Pb	27.0	44.0	5.0	14.0	14.0	12.0	35.0	30.0	24.0	15.0	18.0	15.0
Th	18.0	20.0	21.7	25.0	17.0	23.0	8.5	22.5	23.1	21.0	24.1	25.6
V	25.0	5.0	4.0	8.0	17.0	19.0	3.0	8.0	7.0	8.0	33.0	34.0
Y	12.0	4.0	39.0	36.0	8.0	12.0	12.0	19.0	20.0	19.0	27.0	23.0
Zn	64.0	32.0	23.0	30.0	17.0	25.0	35.0	41.0	24.0	26.0	31.0	39.0
Zr	130.0	100.0	110.0	130.0	116.0	124.0	42.0	87.0	92.0	109.0	162.0	156.0
Be	3.0	3.0	2.0	4.0	3.0	3.0	5.0	2.0	2.0	22.0	2.0	22.0
Co	8.1	2.9	1.6	2.3	3.2	3.8	2.4	2.5	1.7	2.5	5.8	7.1
Cs	4.6	3.3	1.4	2.9	0.7	1.0	2.7	3.5	1.8	2.9	1.3	2.1
Cu	12.0	4.0	3.0	8.0	6.0	7.0	1.0	4.0	2.0	4.0	4.0	7.0
Hf	4.6	3.9	2.6	4.9	4.6	4.4	2.6	3.1	2.2	3.0	4.1	4.0
Mo	4.0	6.0	5.0	9.0	16.0	6.0	4.0	8.0	8.0	8.0	7.0	6.0
Sc	5.4	2.0	3.0	4.6	3.3	5.1	1.3	2.6	2.2	2.6	6.1	6.7
Ta	0.9	0.6	0.3	1.6	0.9	1.5	1.3	1.0	0.7	1.4	0.7	1.1
U	5.9	2.3	1.8	4.6	2.0	3.2	3.7	3.5	3.1	6.1	4.6	4.4
CIPW NORMS												
qz	38.90	33.51	32.91	31.94	28.33	30.62	30.22	31.08	32.98	31.01	30.96	25.83
c	3.52	1.60	0.19	0.84	1.03	0.58	1.12	0.49	0.66	0.44	1.10	0.00
or	22.46	27.42	27.07	27.66	23.17	24.82	30.26	25.71	26.06	26.12	27.13	25.12
ab	21.32	27.42	31.73	31.14	33.34	31.99	28.94	30.55	30.12	31.73	29.87	24.88
an	4.97	6.03	4.63	4.14	8.71	6.92	4.90	0.96	6.09	6.31	4.75	14.12
wo	-	-	-	-	-	-	-	-	-	-	-	0.00
di-di	-	-	-	-	-	-	-	-	-	-	-	0.73
di-he	-	-	-	-	-	-	-	-	-	-	-	0.34
hy-en	2.19	0.70	0.50	0.45	1.05	0.95	0.55	0.95	0.87	0.65	0.95	2.90
hy-fo	3.51	1.44	0.00	2.12	0.84	0.83	0.24	0.21	0.00	0.00	0.00	1.58
mt	0.42	0.10	1.32	0.61	1.26	1.30	0.25	1.75	1.61	1.18	1.25	1.75
il	0.42	0.15	0.32	0.23	0.34	0.30	0.15	0.36	0.34	0.28	0.34	0.65
he	-	-	0.22	-	0.00	-	-	-	0.12	0.33	0.37	-
ap	0.28	0.19	0.12	0.19	0.19	0.19	0.09	0.28	0.17	0.14	0.17	0.21

Table 1. Continued.

Map No.	29	30	37	38	39	40	41	42	43	44	45	46
Field No.	SR-28-1	J-3	SR-29-2	SR-29	SR-28	J-71	SR-18	SR-20	SR-21	SR-22	O-03	O-05
Rock type	CBG	CBG	CBG	CBG	CBG	CBG	AFG	AFG	AFG	AFG	AFG	AFG
SiO_2	67.42	69.33	73.14	74.20	72.70	73.29	77.12	76.30	75.22	73.22	75.83	75.09
TiO_2	0.34	0.29	0.20	0.06	0.16	0.20	0.05	0.04	0.06	0.04	0.09	0.06
Al_2O_3	14.29	13.96	13.61	13.86	15.02	13.80	12.66	13.00	12.74	12.58	12.24	12.64
Fe_2O_3	1.64	1.67	0.58	0.38	0.38	0.75	0.50	0.72	0.80	0.84	1.22	0.92
FeO	1.60	1.05	1.29	0.65	1.24	1.10	0.61	0.45	0.65	0.58	0.29	0.45
MnO	0.06	0.04	0.05	0.04	0.06	0.06	0.02	0.02	0.04	0.04	0.02	0.02
MgO	1.47	1.08	0.37	0.10	0.36	0.42	0.01	0.02	0.08	0.12	0.06	0.04
CaO	2.77	2.41	1.50	0.60	1.44	1.64	0.40	0.36	0.44	0.76	0.57	0.56
Na_2O	3.13	2.91	3.60	3.72	3.50	3.69	4.10	4.30	4.24	4.18	4.14	4.19
K_2O	4.24	4.61	4.25	4.76	4.48	4.21	4.34	4.28	4.24	4.52	4.30	4.34
P_2O_5	0.10	0.10	0.07	0.04	0.12	0.07	0.06	0.04	0.04	0.08	0.03	0.03
LOI	1.66	0.85	0.88	0.70	0.70	0.64	0.31	0.34	0.36	0.68	0.39	0.54
Total	98.72	98.30	99.54	99.11	100.16	99.87	100.18	99.87	98.91	97.64	99.18	98.88
Ba	666.0	736.0	558.0	182.0	678.0	629.0	31.0	30.0	24.0	40.0	81.0	80.0
Rb	153.0	176.0	219.0	330.0	231.0	186.0	449.0	641.0	719.0	422.0	593.0	675.0
Sr	308.0	238.0	202.0	36.0	176.0	226.0	8.0	8.0	2.0	18.0	17.0	16.0
Cr	147.0	93.0	103.0	67.0	87.0	100.0	71.0	74.0	70.0	81.0	129.0	131.0
Ga	21.0	25.0	24.0	22.0	20.0	20.0	28.0	27.0	29.0	30.0	40.0	41.0
Nb	15.0	14.0	16.0	29.0	16.0	15.0	53.0	74.0	81.0	60.0	77.0	75.0
Ni	50.0	39.0	37.0	30.0	33.0	39.0	38.0	36.0	24.0	28.0	41.0	44.0
Pb	10.0	28.0	19.0	35.0	21.0	24.0	29.0	55.0	42.0	34.0	34.0	36.0
Th	21.6	22.7	27.0	17.0	26.0	24.5	43.0	65.0	73.0	51.0	53.0	50.0
V	37.0	9.0	8.0	2.0	13.0	9.0	2.0	1.0	1.0	1.0	2.0	2.0
Y	29.0	20.0	22.0	36.0	260.0	22.0	80.0	120.0	116.0	88.0	98.0	102.0
Zn	39.0	37.0	25.0	20.0	66.0	36.0	51.0	50.0	67.0	48.0	36.0	37.0
Zr	158.0	112.0	103.0	30.0	140.0	114.0	144.0	224.0	202.0	154.0	230.0	186.0
Be	2.0	2.0	3.0	8.0	5.0	22.0	13.0	10.0	12.0	12.0	5.0	4.0
Co	7.8	2.7	2.6	1.9	2.8	2.5	1.4	1.4	1.2	1.3	1.5	1.5
Cs	1.8	3.0	5.1	5.0	6.2	2.2	11.0	11.0	15.0	5.4	7.6	9.0
Cu	50.0	5.0	4.0	3.0	7.0	3.0	4.0	5.0	2.0	5.0	3.0	4.0
Hf	3.7	2.9	2.8	3.6	3.7	2.0	7.9	12.0	15.0	8.8	10.2	9.4
Mo	9.0	7.0	11.0	2.0	8.0	7.0	12.0	7.0	2.0	6.0	10.0	9.0
CIPW NORMS												
qz	24.77	28.20	31.61	32.63	31.08	31.23	35.65	34.12	33.15	30.07	34.23	32.38
c	0.00	0.04	0.53	1.59	2.08	0.36	0.63	0.73	0.47	-	-	-
or	25.06	27.24	25.12	28.13	26.48	24.88	25.65	25.29	25.06	26.71	25.41	25.65
ab	26.49	24.62	30.46	31.48	29.62	31.23	24.69	36.39	35.88	35.37	35.03	36.3
an	12.42	11.30	6.98	2.72	6.36	7.68	1.59	1.52	1.92	2.21	1.84	2.42
wo	-	-	-	-	-	-	-	-	-	-	0.16	-
di-di	0.42	-	-	-	-	-	-	-	-	0.41	0.32	0.13
di-he	0.11	-	-	-	-	-	-	-	-	0.45	-	-
hy-en	3.47	2.69	0.92	0.25	0.90	1.05	0.02	0.05	0.2	0.11	-	0.04
hy-fo	1.07	0.14	1.65	0.85	1.81	1.18	0.66	0.2	0.51	0.14	-	-
mt	2.38	2.42	0.84	0.55	0.55	1.09	0.72	1.04	1.16	1.22	0.74	1.33
il	0.65	0.55	0.38	0.11	0.30	0.38	0.09	0.08	0.11	0.08	0.17	0.11
he	-	-	-	-	-	0.00	-	-	-	-	0.71	-
ap												

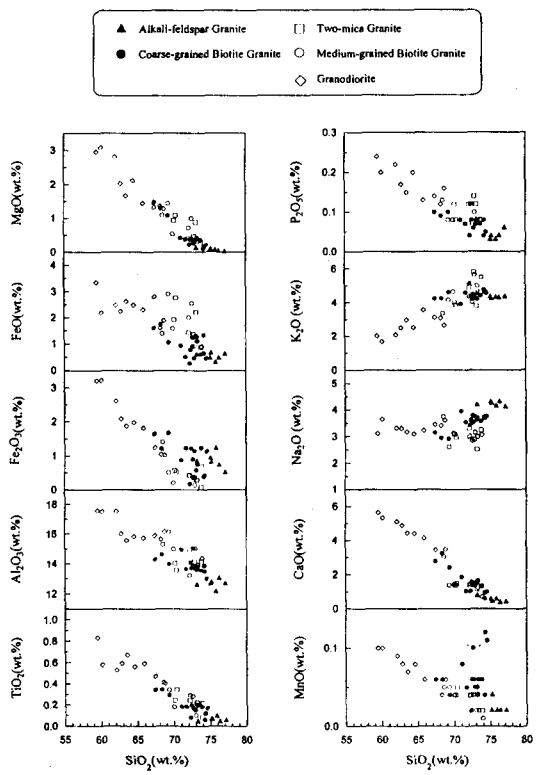

Fig. 3. Abundances of major elements plotted against SiO_2 contents for the granitic rocks in the study area.

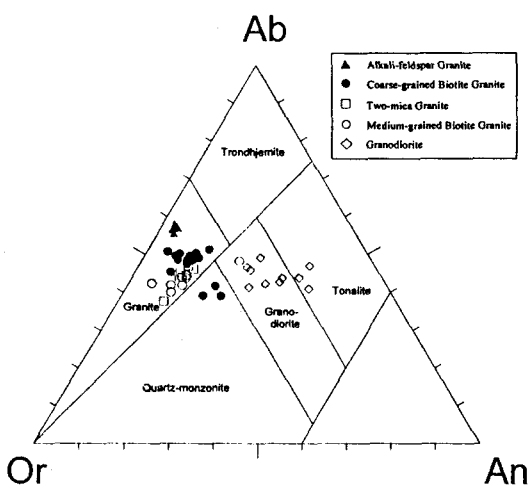

Fig. 4. Normative Albite(Ab)-Orthoclase(Or)-Anorthite(An) diagram for the granitic rocks in the study area(After O'Connor, 1965).

magma. A normative Or-An-Ab diagram for the granitic rocks in the area distinguishes

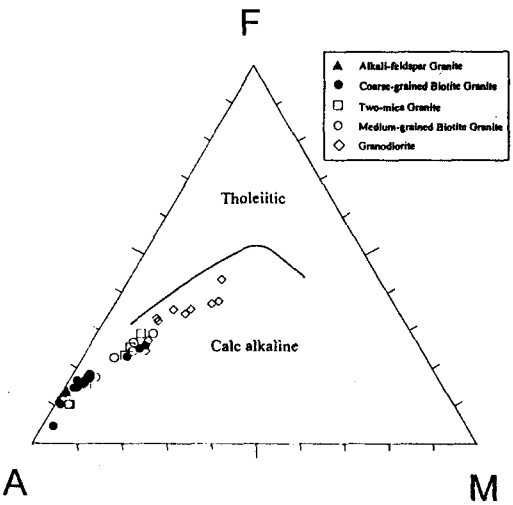

Fig. 5. AFM diagram for the granitic rocks in the study area(Irvine and Baragar, 1971).

granodiorite in a granodiorite and tonalite domain from biotite granite, two-mica granite and alkali feldspar granite in a granite domain (Fig. 4). Granitic rocks display a calc-alkaline trend in the AFM diagram (Fig. 5). In the well-known ACF diagram, granodiorite and alkali feldspar granite are plotted in the field of I-type, whereas two-mica granite of and biotite granite of both I- and S-type granitic rocks (Fig. 6). As shown in the discrimination diagrams of magnetite- and ilmenite-series granitic rocks (Fig. 7), granodiorite and alkali feldspar granite are plotted in the field of magnetite-series, two-mica granite in the ilmenite-series, and biotite granite is scattered in both fields.

Abundances of Ba, Sr and Sc shows a strong depletion pattern with the increase of SiO_2 content, while those of Rb, Nb, Th and U vary in an enrichment trend (Fig. 8). Contents of Y, Zr and Ga are dispersed. The tectonic discrimination diagrams proposed by Pearce *et al.* (1984) suggest that the granitic rocks in the study area are classified as volcanic arc and syn-collisional granites except alkali feldspar granite as within-plate granite (Fig. 9). The chondrite-normalized REE patterns for the

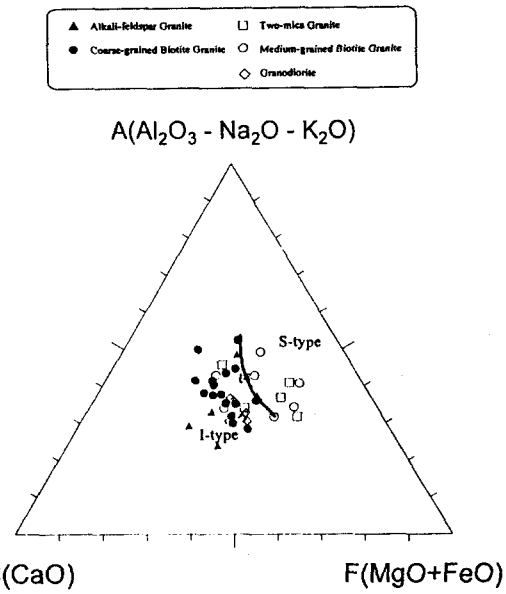

Fig. 6. I- and S-type granite classification diagrams (Hine *et al.*, 1978).

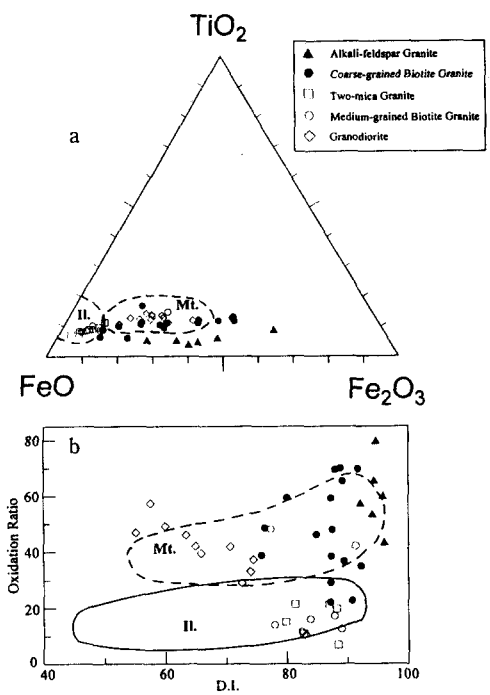

Fig. 7. Magnetite-(Mt.) and Ilmenite-series(Il.) granitoid classification diagrams.
a) TiO_2-FeO-Fe_2O_3 diagram.
b) D.I.(Differentiation Index) vs Oxidation Ratio for the granitic rocks in the study area.

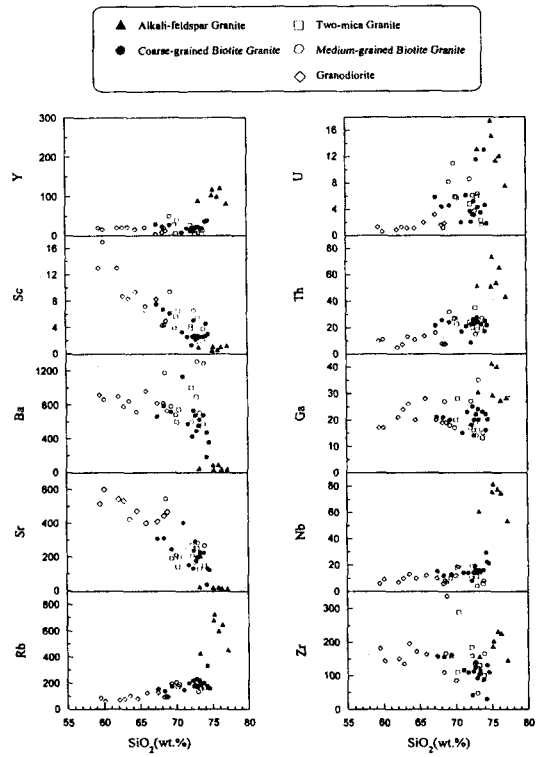

Fig. 8. Trace element concentrations(ppm) plotted against SiO_2 contents for the granitic rocks in the study area.

granitic rocks are shown in Fig. 10. Granodiorite shows a relatively uniform pattern with almost no Eu anomalies and relatively high $(La/Lu)_{CN}$ ratios. Biotite granite and two-mica granite show relatively wider but generally similar patterns except moderately negative Eu anomalies compared with granodiorite. Alkali feldspar granite exhibits a characteristic pattern of V-shaped flat wing-type with low $(La/Lu)_{CN}$ ratios of 1.20-2.19 and excessively negative Eu anomalies.

Rb-Sr ISOTOPE SYSTEMATICS

Sr isotopic compositions of the representative samples were determined at the Korea Basic Science Center (Table 2). A plot of $^{87}Rb/^{86}Sr$-$^{87}Sr/^{86}Sr$ for the granitic rocks in the study area does not form a single isochron but shows

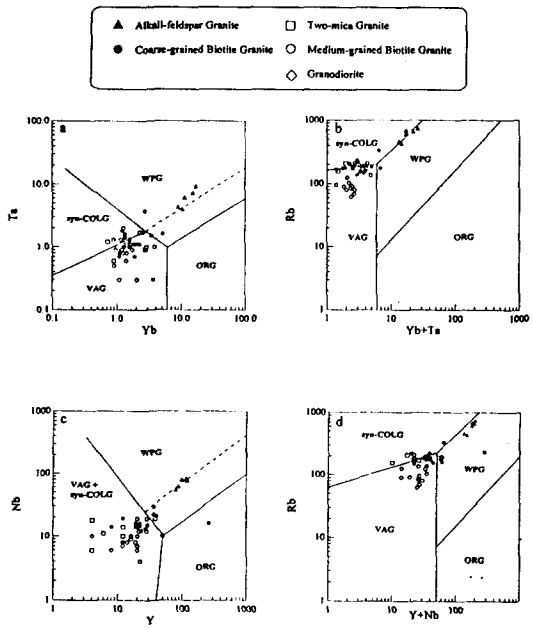

Fig. 9. Plots for granitic rocks on the discrimination diagrams of Pearce *et al.*(1984).
VAG : Volcanic Arc Granites, WPG : Within-Plate Granites, syn-COLG : syn-Collisional Granites, ORG : Ocean Ridge Granites.

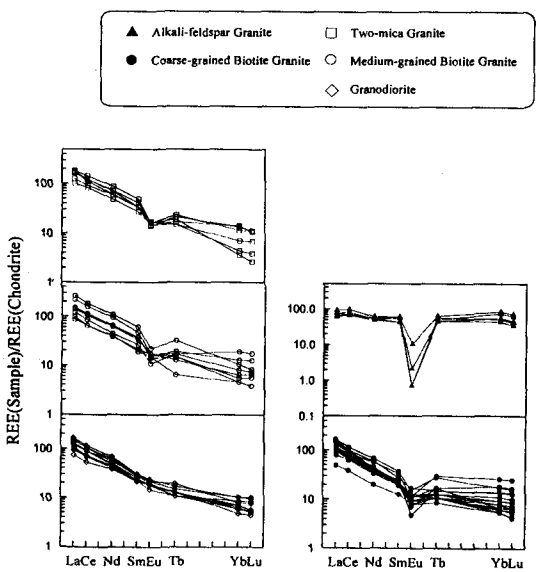

Fig. 10. REE abundances normalized to chondrites for the granitic rocks in the study area.

three linear trends; one for samples of granodiorite, biotite granite and two-mica granite from northwestern area indicates an age of 899±67 Ma and a Sr initial ratio of 0.70727±0.00060, another for some biotite granite samples from southeastern area yields an age of 318±38 Ma with an initial ratio of 0.7063±0.0011, the other for the other biotite granite samples from southeastern area exhibits an age of 125.6±4.4 Ma and an initial ratio of 0.70940±0.00011 (Fig. 11). These trends are separated depending on geographical locations rather than on petrographic characteristics, which suggests that the Sr isotopic compositions of the granitic rocks have been locally affected by Precambrian basements. Alkali feldspar granite samples, even though only three measurements, are plotted irregularly in the $^{87}Rb/^{86}Sr$-$^{87}Sr/^{86}Sr$ diagram, and so do not form any meaningful isochron, which indicates the alkali feldspar granite was originally heterogeneous in Sr isotopic composition or has been isotopically disturbed since its emplacement.

AGE OF EMPLACEMENT

The granitic rocks in the study area and hornblende-biotite granodiorite and porphyritic biotite granite in the Inje-Hongcheon district, southwest of this study area, were formerly grouped into the Cretaceous Bulgugsa granite (KIER, 1983). However, recent geochemical studies (Jwa, 1990; Jwa, 1991; Jwa *et al.*, 1990) suggested that all the granitic rocks from the Inje-Hongcheon district have been formed during late Triassic to early Jurassic period on the basis of the Rb-Sr whole rock isochron of 212±26.6 Ma for hornblende-biotite granodiorite and explained the Sr isotopic inhomogeneities in equigranular, porphyritic and two-mica granites in terms of wall-rock assimilation as well as fractional crystallization in a magma chamber. According to these studies of Jwa and his colleagues, nowadays all the granitic rocks distributed in the northeastern part of the Kyeonggi massif are classified as the Daebo granite.

Three ages for the granitic rocks in the

Table 2. Elemental abundances of Rb and Sr, and ratios of $^{87}Rb/^{86}Sr$ and $^{87}Sr/^{86}Sr$.

MAP NO.	TYPE[1)]	Rb(ppm)	Sr(ppm)	$^{87}Rb/^{86}Sr$	$^{87}Sr/^{86}Sr$[2)]
1	GD	103	425	0.702	0.71687±0.000007
2	GD	123	400	0.891	0.71723±0.000006
3	GD	62	600	0.299	0.71162±0.000006
4	GD	90	444	0.587	0.71513±0.000006
8	GD	125	410	0.883	0.71780±0.000006
9	GD	85	515	0.478	0.71241±0.000014
11	MBG	184	168	3.18	0.75206±0.000006
21	MBG	207	196	3.06	0.73050±0.000006
34	TMG	175	270	1.88	0.72755±0.000007
35	TMG	170	130	3.80	0.76003±0.000007
15	CBG	174	130	3.88	0.71609±0.000007
16	CBG	147	402	1.06	0.71131±0.000007
23	CBG	220	132	4.83	0.73124±0.000009
26	CBG	173	199	2.52	0.71895±0.000006
27	CBG	198	152	3.78	0.72260±0.000007
38	CBG	330	36	26.7	0.75808±0.000007
39	CBG	231	176	3.80	0.72073±0.000006
42	AFG	641	8	245	1.29844±0.000025
44	AFG	422	18	69.3	0.92395±0.000008
46	AFG	675	16	128	1.18986±0.000008

[1)] GD:Granodiorite, MBG:Medium-grained Biotite Granite, TMG:Two-mica Granite, CBG:Coarse-grained Biotitie Granite, AFG:Alkali Feldspar Granite [2)] Normalized to $^{86}Sr/^{88}Sr=0.1194$. Measured $^{87}Sr/^{86}Sr$ of NBS987 : 0.710223±0.000006

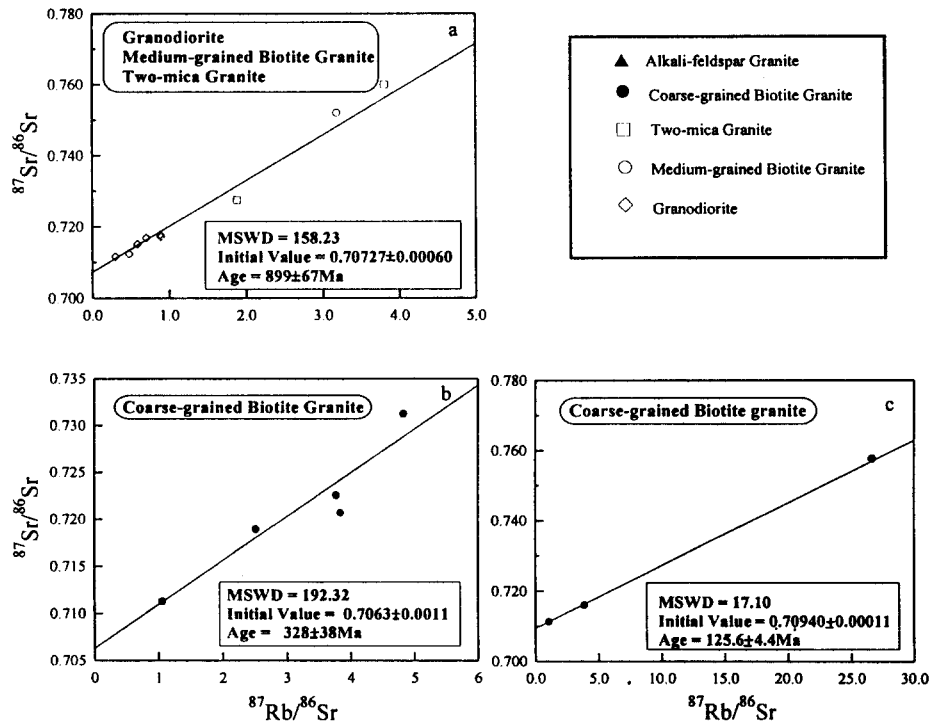

Fig. 11. Rb-Sr isochrons for the granitic rocks in the study area.

Table 3. Summary of published fission track, K-Ar and Rb-Sr ages for the granitic rocks in the Inje area.

No. in Fig. 2	Geological Age[1)]	F.T. Age(Ma)±1σ[2)]	K-Ar Age(Ma)±1σ[3)]	Rb-Sr Age(Ma)±1σ[4)]	National Grid
ⓐ	Cretaceous	40.5±5.4	129.5±6.5	129±1.4	(1553, 5082)
ⓑ	Cretaceous	57.4±6.6	91.1±4.5	71±0.5	(1489, 5099)
ⓒ	Cretaceous		82.6±4.0		(1477, 5106)
ⓓ	Cretaceous		86.0±4.0	123±0.1	(1453, 5116)
ⓔ	Cretaceous	62.5±3.8	100.1±5.0	127±2.1	(1402, 5133)

[1)] Geological ages adopted from Lee(1982) and the geological map of Korea (1:250,000), Jangjeon sheet and Chuncheon sheet (GMIK, 1973).
[2)] Fission track ages of apatite from Jin et al.(1984) [3)] K-Ar ages of biotite from Jin et al.(1984)
[4)] Rb-Sr ages of two points for whole rock and biotite from Choo et al.(1982)

study area are calculated from linear trends in the plot of $^{87}Rb/^{86}Sr$-$^{87}Sr/^{86}Sr$ (Fig. 11). The ages of 899±67 Ma and 318±38 Ma are too old to be considered as an age of emplacement for the granitic rocks in this area. Former published radiometric ages determined from the samples mainly along the road of No. 44, Wontong through Yangyang, passing the Hangyeryeong, indicate the possibility of the Cretaceous as an emplacement age of granitic rocks in this area (Table 3). With reference of the formerly dated ages, an age of 125.6±4.4 Ma calculated by the slope in the plot of $^{87}Rb/^{86}Sr$-$^{87}Sr/^{86}Sr$ for biotite granite samples from southeastern area can be accepted as a reasonable emplacement age. Apart from the Inje-Hongcheon district, the granitic rocks in the vicinity of the Mt. Sorak might be emplaced during the Cretaceous period rather than the Jurassic period.

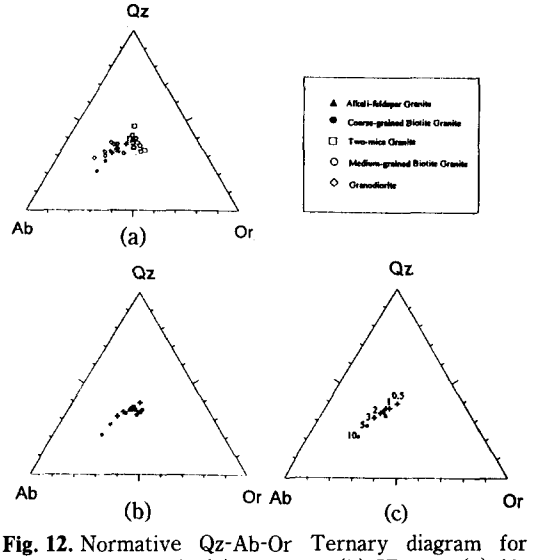

Fig. 12. Normative Qz-Ab-Or Ternary diagram for the granitic rocks in (a) NW area, (b) SE area, (c) Alkali feldspar granite.
Bold pluses indicate isobaric minimum and bold circles indicate isobaric eutectic at various P_{H2O}(Kb) [Numbers shown in (c)] (Afer Luth *et al.*, 1964).

AFC MODEL

As shown in the Harker's diagram (Fig. 3 and Fig. 8), the variations in major and some trace elemental abundances with the increase of SiO_2 contents show a typical differentiation trend of fractional crystallization in a granitic magma. In the normative Qz-Ab-Or diagrams for the granitic rocks in the area (Fig. 12), granodiorite forms a roughly linear trend whose extension meets approximately the Ab corner, and medium-grained biotite granite and two-mica granite show a common trend extended to the $Ab_{25}Or_{75}$ point on the Ab-Or boundary. Sr and Ba have pretty low correlation for granodiorite but highly positive correlation for the others (Fig. 13). These features can be explained in terms of fractional crystallization model, whereby a granitic magma was evolved mainly through fractionation of feldspars, plagioclase and alkali feldspar in the early stage (granodiorite) and then dominantly

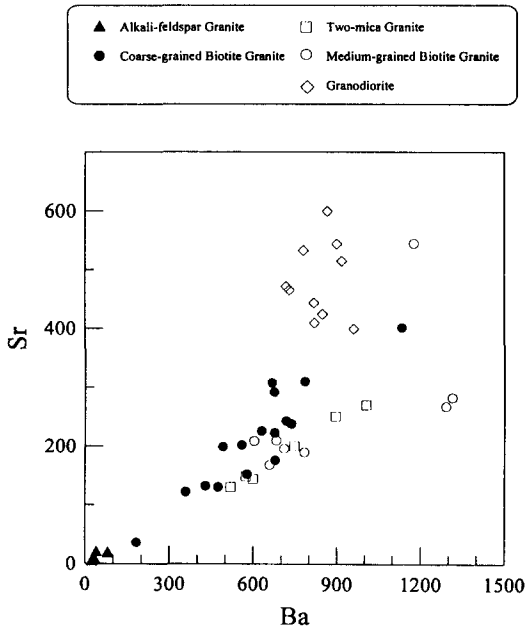

Fig. 13. Correlation diagram of Sr and Ba.

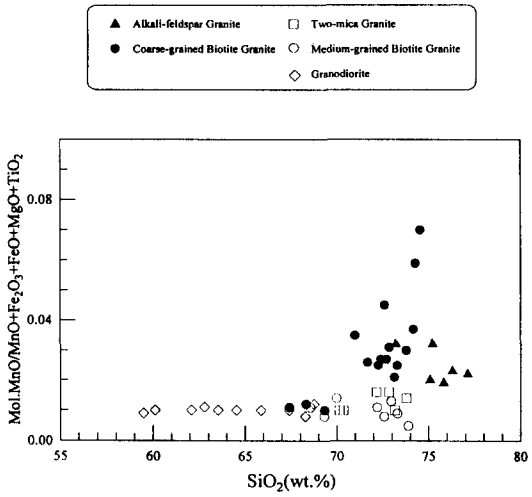

Fig. 14. SiO_2(wt.%) vs Mol. MnO/(MnO+FeO+MgO+TiO_2) diagram for the granitic rocks in the study area.

alkali feldspar in the later stage (biotite granite and two-mica granite) (e.g. McCarthy and Hasty, 1976; Hanson, 1978). Some trace elements such as Ba, Zr, Ga, Nb and U are strongly dispersed. Since variations in trace elements are much more sensitive to source materials and environments of partial melting or crystallization, a dispersed pattern of trace elemental abundances is usual in an igneous system. In the study area, biotite granites in marginal areas show generally wider dispersions of elemental contents than granodiorite in the central zone, which can be explained by contamination of outer metasedimentary basement. A steep increase in the ratio of MnO/($MnO+Fe_2O_3+FeO+MgO+TiO_2$) (mol) for the biotite granite, especially in the southeastern area (Fig. 14), supports contamination as an example in the batholiths of California (Auge and Brimhall, 1988). The additional contaminants of metasediments into granitic magma might not have drastically changed the major elemental composition of the fractionating system (McBirney, 1979; Pitcher, 1993). Migmatitic rocks distributed in the marginal area supports local assimilation.

A coupled assimilation - fractional crystallization (AFC) model favorably accounts for variations in elemental abundances and isotopic ratios for the granitic suite. General equations describing both isotopic effects and trace element effects for a general model of concurrent assimilation and fractional crystallization derived by DePaolo (1981) have been widely applied to igneous problems. Using DePaolo's equation, the variations of the radiogenic isotopic ratios affected by assimilation and fractional crystallization can be simply represented in terms of the reciprocal elemental concentration as the Equation (1), which can be rewritten as the Equation (2).

$$\frac{\varepsilon_m - \varepsilon_m^o}{\varepsilon_a - \varepsilon_m^o} = \frac{1/C_m - 1/C_m^o}{(r+D-1)/rC_a - 1/C_m^o} \quad (1)$$

ε_m : isotope ratio in magma
ε_m^o : isotope ratio in original magma
ε_a : isotope ratio in contaminant
C_m : elemental concentration in magma
C_o^m : elemental concentration in original magma
C_a : elemental concentration in contaminant
D : bulk solid/liquid distribution coefficient

for the element

r : ratio of assimilation rate over crystallization rate

$$\frac{\varepsilon_m - \varepsilon_m^o}{1/C_m - 1/C_m^o} = \frac{\varepsilon_a - \varepsilon_m^o}{(r+D-1)/rC_a - 1/C_m^o} \quad (2)$$

The Equation (2) shows that a plot of isotopic ratio ε versus reciprocal concentration of magma $1/C_m$ yields a straight line with a slope depending on the ratio (r) of assimilation rate/fractional crystallization rate and the bulk distribution coefficient (D) for the element. For simple mixing, in a case of $r=\infty$ or D=1, the above Equation (2) reduces to;

$$\frac{\varepsilon_m - \varepsilon_m^o}{1/C_m - 1/C_m^o} = \frac{\varepsilon_a - \varepsilon_m^o}{1/C_a - 1/C_m^o} \quad (3)$$

which shows a simple straight mixing line connecting two points for the original magma and the contaminant (Vollmer, 1976; Langmuir *et al.*, 1978). The AFC model falls on the linear line connecting two points $(1/C_m^o, \varepsilon_m^o)$ and $((r+D-1)/rC_a, \varepsilon_a)$. For strontium isotopes, the Equation (3) can be applied as;

$$\frac{(^{87}Sr/^{86}Sr)_m - (^{87}Sr/^{86}Sr)_m^o}{1/Sr_m - 1/Sr_m^o} = \frac{(^{87}Sr/^{86}Sr)_a - (^{87}Sr/^{86}Sr)_m^o}{(r+D-1)/rSr_a - 1/Sr_m^o} \quad (4)$$

From the Equation (4), the relationship of fractional crystallization (FC), simple mixing and assimilation - fractional crystallization (AFC), can be simplified in a graph of initial $^{87}Sr/^{86}Sr$ versus 1/Sr (Fig. 15). The figure of initial $^{87}Sr/^{86}Sr$ ratios calculated by assuming the emplacement age of 125 Ma versus reciprocal Sr concentrations show distinctively two linear groups with some exceptive scatter, one for granodiorite, biotite granodiorite and two-mica granite in the northwestern area and the other for biotite granite in the southeastern area (Fig. 16). Both lines meet around the point of granodiorite, which can be regarded as

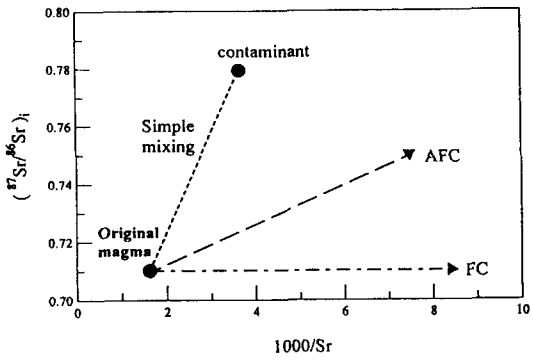

Fig. 15. AFC model.

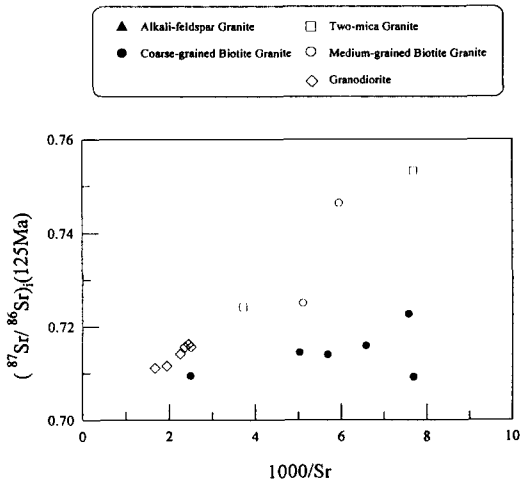

Fig. 16. 1000/Sr vs initial $^{87}Sr/^{86}Sr$ ratio diagram for 125 Ma.

primitive in this area. Differences in slopes of two linear groups might be results of different contaminants (different values of $(^{87}Sr/^{86}Sr)_a$ and Sr_a) or/and more favorably unequal ratios (r) of assimilation rate over crystallization rate, in other words, unequal degree of contamination during crystallization. Generally, it can be inferred that the granitic rocks in the northwestern area might have been more highly contaminated by the surrounding metasediments having higher $^{87}Sr/^{86}Sr$ ratios, compared with those in the southeastern area. Also $^{87}Sr/^{86}Sr$ and Rb/Sr shifts in a magma affected by assimilation and fractional crystallization yield "pseudoisochrons", which give

meaningless ages, 899±67 Ma and 318±38 Ma, significantly older than the inferred geological age, the Cretaceous period.

EVOLUTION OF GRANITIC MAGMAS

The granitic rocks in the study area show characteristics of reverse zoning, distribution of granodiorite in the central zone and biotite granite to two-mica granite in the marginal zone. Also, granodiorite and most biotite granite in the southeastern area represent I-type and magnetite-series characteristics, while most biotite granite and two-mica granite in the northwestern area exhibit S-type and ilmenite-series ones. The reverse zoning, i.e. relatively more silicic in the outer zone, can be explained by a large scale convecting model, whereby progressively more silicic magma is evolved in the convecting part, while relatively mafic magma of early stage is unchanged in the static zone existing at the upper and/or interior part. In the convecting zone, fractionation and convection occurred from the inner part toward the outer part, changed the magma more silicic and reaction with the surrounding Precambrian metasediments in the more reducing environment at the contact to be S-type and ilmenite-series in the northwestern area (Shaw, 1965; Shimizu, 1986; Jwa, 1990). The inferred initial $^{87}Sr/^{86}Sr$ ratio, 0.709, of the primitive magma at 125 Ma and I-type characteristics suggest that the magma have been generated by partial melting of igneous originated crustal materials and eventually solidified to form the granitic rocks in this area through assimilation and fractional crystallization.

Alkali feldspar granite shows characteristics distinct from the other granitic rocks in this district, such as significantly high and scattered $^{87}Sr/^{86}Sr$ ratio (0.9239-1.1331), anomalous enrichment of HFSE (high field strength elements), heavy REE and incompatible elements (e.g. Rb), severe depletion of compatible elements (Sr, Ba and etc.), and highly negative(-) Eu anomaly. These characteristics are very similar to those of well-known A-type granites (Loiselle and Wones, 1979; Collins *et al.*, 1982; Whalen, *et al.*, 1987) but can not be explained simply by a single process in connection with other granitic rocks. Hydrothermal alteration can be considered as a possible hypothetical process for the evolution of alkali feldspar granite. About 125 Ma, the primary magma was evolved to solidify biotite granite and at the latest stage, the evolved hydrothermal solution reacted with the formerly solidified biotite granite resulting in alteration to form alkali feldspar granite. And later, about 55Ma, which are inferred from fission track apatite dating (Table 3) and Rb-Sr whole rock isochron for the granitic porphyry (Kim, 1995), the alkali feldspar granite was again affected by local igneous activities.

CONCLUDING REMARKS

The granitic rocks widely distributed in the vicinity of the Mt. Sorak, the northeastern part of the NE-SW elongated Mesozoic batholith in the Kyeonggi massif, consist petrographically of granodiorite, biotite granite, two-mica granite and alkali feldspar granite. An age of 125.6±4.4Ma calculated by the slope in the plot of $^{87}Rb/^{86}Sr$-$^{87}Sr/^{86}Sr$ for the biotite granite samples (even though only three points) from the southeastern area, supported by the formerly dated radiometric ages (Jin *et al.*, 1984), can be considered as an emplacement age of the granitic rocks in the study area. This age is much younger than the age of 212±26.6 Ma obtained from a Rb-Sr whole rock isochron for the hornblende-biotite granodiorite in the Inje-Hongcheon district (Jwa, 1990).

On the basis of elemental variations and Sr isotope compositions, an evolutional model for the granitic magmas in this area is proposed as follows. The primary magma of I-type and magnetite-series, was generated by partial melting of igneous originated crustal materials and eventually solidified to form the granitic

rocks in the study area through assimilation and fractional crystallization. In the outer convecting zone, the residual melts became more silicic granitic magma of S-type and ilmenite-series through convection from the inner part toward the outer part and reaction with the surrounding Precambrian metasediments in the more reducing environment at the contact. A hypothetical model of hydrothermal alteration for the anomalous alkali feldspar granite can be considered for the evolution of alkali feldspar granite. About 125 Ma, the primary magma was evolved to solidify biotite granite and at the latest stage, the evolved hydrothermal solution probably reacted with the formerly solidified biotite granite to form alkali feldspar granite, and probably later the alkali feldspar granite was again affected by local igneous activities.

ACKNOWLEDGEMENT

This study was supported by the Korea Science and Engineering Foundation (KOSEF 911-0503-004-02). This paper has benefited from the constructive comments of Drs. Lee, J.I., Jwa, Y.J. and an anonymous reviewer. Helpful assistances in field and laboratory works by Dr. Chin Ho-Ill, Mr. Yim Gil-Jae and Mr. Cheong Yeon-Tai are greatly appreciated.

REFERENCES

Ague, J.J. and Brimhall, G.H., 1988, Regional variations in bulk chemistry, mineralogy, and the compositions of mafic and accessory minerals in the batholiths of California. Geol. Soc. Amer. Bull., 100, 891-911.

Choo, S.H., Jin, M.S., Yoon, H.S. and Kim, D.H., 1982, Rb/Sr age determinations on granite gneiss and granite in Seosan, Onjeongri granite, and Mesozoic granites along the east coast, Korean peninsular. Rept. Geol. Mineral. Res., 13, KIER., 193-208.

Collins, W.J., Beams, S.D., White, A.J.R. and Chappell, B.W., 1982, Nature and origin of A-type granites with particular reference to southeastern Australia. Contrib. Mineral. Petrol., 80, 189-200.

DePaolo, D.J., 1981, Trace element and isotopic effects of combined wallrock assimilation and fractional crystallization. Earth Planet. Sci. Lett., 53, 189-202.

GMIK (Geological and Mineral Institute of Korea), 1973, Geological map of Korea (1:250,000). GMIK, Jangjeon and Chuncheon, Korea.

Hanson, G.N., 1978, The application of trace elements to petrogenesis of igneous rocks of granitic composition. Earth Planet. Sci. Lett., 38, 26-43.

Hine, R. and Williams, I.S., Chappell, B.W. and White, A.J.R., 1978, Contrast between I-type and S-type granitoids of the Kosciusko batholith. Jour. Geol. Soc. Australia, 25, 219-234.

Irvine, T.N. and Baragar, W.R.A., 1971, A guide to the chemical classification of the common volcanic rocks. Can. J. Earth Sci., 8, 523-548.

Ishihara, S., 1977, The magnetite-series and ilmenite-series granitic rocks. Mining Geol., 27, 293-305.

Jin, M.S., Gleadow, A.W.J., and Lovering, J.F., 1984, Apatite fission track dating from the Jurassic and Cretaceous granites in South Korea. J. Geol. Soc. Korea, 20, 257-265.

Jwa, Y.J., 1990, Petrography and major element geochemistry of the granitic rocks in the Inje-Hongcheon district, South Korea. J. Min. Petrol. Econ. Geol., 85, 98-112.

Jwa, Y.J., 1991, A study on Jurassic granitic rocks in the Inje-Hongcheon district, South Korea. II. Effect of wallrock assimilation. J. Geol. Soc. Korea, 27, 13-23.

Jwa, Y.J., Nakazima, T., Uchiumi, S. and Shibata, K., 1990, Geochronology and cooling history of Mesozoic granitic rocks in the Inje-Hongcheon district, South Korea. Geochem. J., 24, 93-103.

KIER (Korea Institute of Energy and Resources), 1983, Geology of Korea, Text for geological map of Korea. 1:1,000,000.

Kim, S.B., 1995, Geochemistry and petrogenesis of the granitic rocks in the vicinity of the Mt. Sorak. Kangwon National Univ. unpublished Ph. D. thesis, 98p.

Langmuir, C.H., Vocke, R.D.,Jr., Hanson, G.N. and Hart, S.R., 1978, A general mixing equation with application to Icelandic basalt. Earth Planet. Sci. Lett., 37, 380-392.

Lee, D.S., 1982, Geology around Mt. Sorak. J. Korean Earth Sci. Educ. Assoc., 3, 41-47.

Loiselle, M.C. and Wones, D.R., 1979, Characteristics and origin of anorogenic granites. Geol. Soc. Amer. Abstr. Prog., 11, 468.

Luth, W.C., Jahns, R.H. and Tuttle, O.F., 1964, The granite system at pressures of 4 to 10 kilobars. J. Geophys. Res., 69, 759-773.

McCarthy, T.S. and Hasty, R.A., 1976, Trace ele-

ment distribution patterns and their relation to the crystallization of granitic melt. Geochim. Cosmochim. Acta, 40, 1351-1358.

McBirney, A.R., 1979, Effects of assimlation. In: H. S. Yoder, Jr. (ed.), The Evolution of the Igneous Rocks. Fiftieth Anniversary Perspectives. Princeton Univ. Press, Princeton, N.J., 307-390.

O'Conner, J.T., 1956, A classification for quartz-rich igneous rocks based on feldspar ratios. U.S. Geol. Surv. Prof. Paper 525-B, 79p.

Pearce, J.A., Harris, N.B.W. and Tindle, A.G., 1984, Trace element discrimination diagram for the tectonic interpretation of granitic rocks. J. Petrol., 25, 956-983.

Pitcher, W.S., 1993, The Nature and Origin of Granite. Chapman and Hall, London, 321p.

Shaw, H.R., 1965, Comments on viscosity, crystal settling, and convection in granitic magmas. Am. J. Sci., 263, 102-152.

Shimizu, M., 1986, The Tokuwa batholith, central Japan - An example of occurrence of ilmenite-series granitoids in a batholith, The University Museum, Univ. of Tokyo Bull., 28, 146p.

Vollmer, R., 1976, Rb-Sr and U-Th-Pb systematics of alkaline rocks: The alkaline rocks from Italy. Geochim. Cosmochim. Acta, 40, 283-295.

Whalen, J.B., Currie, K.L. and Chappell, B.W., 1987, A-type granites: Geochemical characteristics, discrimination and petrogenesis. Contrib. Mineral. Petrol., 95, 407-419.

White, A.J.R. and Chappell, B.W., 1983, Granitoid types and their distribution in the Lachlan fold belt, southeastern Australia. Geol. Soc. Am. Mem., 159, 21-33.

(책임편집:좌용주)

설악산 부근의 화강암류에 대한 지구화학 및 성인

민경원[1] · 김성범[2]

[1]강원대학교 공과대학 자원공학과, [2]쌍용 자원개발 주식회사 (deceased on Feb. 10, 1996)

요 약 : 경기육괴 내에 북동-남서 방향으로 넓게 분포하는 대규모의 중생대 화강암저반의 북동부지역인 설악산 부근의 화강암류는 화강섬록암, 흑운모화강암, 복운모화강암 및 알카리장석화강암으로 대별된다. 화강암류들의 주원소 및 미량원소의 함량변화 양상은 화강암질 마그마에서의 전형적인 분화경향을 나타낸다. 전체적으로 칼크-알카리계열로서, 화강섬록암 및 남동부의 흑운모화강암은 I-형/자철석계열에 속하며, 북서부의 흑운모화강암 및 복운모화강암은 S-형/티탄철석계열의 특성을 나타낸다. 경기육괴의 북동부에 분포하는 화강암류는 최근 인제-홍천지역의 화강암류에 대한 연대측정 연구에 의하여 모두 후기 트리아스기 내지 초기 쥬라기의 대보화강암류로 분류되어 왔다. 본 연구에서는, 기존의 설악산지역에서 얻어진 연대를 토대로, 연구지역의 남동부 흑운모화강암에 대한 $^{87}Rb/^{86}Sr$-$^{87}Sr/^{86}Sr$의 기울기에 의하여 얻어진 연대인 125.6±4.4 Ma를 화강암의 관입연대로 해석하고, 연구지역에서의 화강암류의 원소함량 및 Sr 동위원소비의 변화를 설명할 수 있는 마그마 진화과정의 추정 모델을 제시하였다. 125 Ma 경에 지각물질의 부분용융에 의하여 생성 관입된 I-형/자철석계열의 초기 마그마 및 분별결정, 대류 및 주변암인 선캠브리아기 변성퇴적암류의 동화에 의하여 S-형/티탄철석계열로 점차 진화된 마그마의 고결로 화강섬록암, 흑운모화강암 및 복운모화강암을 형성하였을 것이다. 마그마의 분화 말기에 형성된 열수는 이미 고결된 흑운모화강암를 알카리화강암으로 변질시키고, 알카리화강암은 후기의 지역적인 화성활동에 의하여 재차 영향를 받았을 것으로 추정된다.

핵심어 : 설악산, 화강암류, 지구화학, 성인, 분별결정, 동화